1521-009X/45/5/449–456$25.00
Drug Metabolism and Disposition

https://doi.org/10.1124/dmd.116.074245
Drug Metab Dispos 45:449–456, May 2017

Correlation between Membrane Protein Expression Levels and Transcellular Transport Activity for Breast Cancer Resistance Protein[S]

Houfu Liu, Liang Huang, Yi Li,[1] Tingting Fu, Xueying Sun, Yan-Yan Zhang, Ruina Gao, Qingfang Chen, Wandong Zhang, Jasminder Sahi,[1] Scott Summerfield, and Kelly Dong

Departments of Mechanistic Safety and Disposition (H.L., T.F., X.S.), Bioanalysis, Immunogenicity and Biomarker (L.H., R.G., K.D.), Protein, Cellular and Structural Sciences (Q.C.), Modeling and Computational Sciences (Y.-Y.Z.), Integrated Biological Platform Sciences (W.Z.), and Drug Metabolism and Pharmacokinetics (Y.L., J.S.), Platform Technology and Science, GlaxoSmithKline R&D China; and Department of Bioanalysis, Immunogenicity and Biomarker (S.S.), Platform Technology and Science, GlaxoSmithKline, Ware, United Kingdom

Received November 8, 2016; accepted February 10, 2017

ABSTRACT

Emerging evidence indicates an important role for the breast cancer resistance protein (BCRP) in limiting brain penetration of substrate drugs. While in vitro transwell assays can provide an indication of BCRP substrate potential, the predictability of these assays in relation to in vivo brain penetration is still under debate. The present study examined the correlation of BCRP membrane protein expression level and transcellular transport activity across Madin-Darby canine kidney (MDCK) II monolayers. We expressed human BCRP or murine BCRP1 in MDCKII wild-type cells using BacMam2 virus transduction. The selective P-glycoprotein (P-gp) inhibitor LY335979 (1 μM) was included in the transport medium to measure BCRP-mediated transcellular transport for P-gp and BCRP cosubstrates. The BCRP levels in membrane extracts from MDCKII-BCRP or MDCKII-Bcrp1 cells were quantified by liquid chromatography–tandem mass spectrometry. The results are summarized as follows: 1) the membrane protein expression levels correlate with the corrected efflux ratios of substrates for human BCRP and murine BCRP1 within the efflux ratios investigated; 2) we demonstrate good concordance in rank order between the BCRP and BCRP1-mediated efflux ratios for 12 drugs; and 3) we propose an approach to contextualize in vitro BCRP transport data of discovery compounds by comparing them to the in vitro and in vivo transport data of the reference drug dantrolene and taking into account interbatch variation in BCRP expression. This approach correctly predicted compromised brain penetration for 25 discovery compounds in rodents, which were BCRP substrates but not P-gp or weak P-gp substrates. These results suggest that BCRP-expressing MDCKII cells are useful in predicting the in vivo role of BCRP in brain penetration.

Introduction

Drugs designed for brain disorders should be able to the cross the blood-brain barrier (BBB) at appropriate concentrations in order to exert their desired pharmacology. The strength of the BBB is the result of very tight junctions between endothelial cells, polarized active efflux transporters, and limited pinocytosis. The major efflux transporters expressed at the luminal side of the BBB are the ATP-binding cassette (ABC) family of transporters including P-glycoprotein [(P-gp); ABCB1] and the breast cancer resistance protein [(BCRP); ABCG2]. The prominent role of P-gp in limiting the entry of various drugs into the central nervous system (CNS) has been well documented (Schinkel et al., 1996; Doran et al., 2005; Shen and Zhang, 2010). Thus, polarized cell monolayers such as Madin-Darby canine kidney (MDCK) or Caco2 with expression of human P-gp were deployed by the pharmaceutical industry to triage drug candidates in CNS drug discovery. The predictive value of these in vitro assays was widely recognized and strong P-gp substrates were unarguably deprioritized for centrally acting compounds (Yamazaki et al., 2001; Mahar Doan et al., 2002; Feng et al., 2008; Kikuchi et al., 2013).

BCRP (ABCG2) is the second member of the G subfamily of ABC transporter proteins. BCRP is constitutively expressed in human tissues such as CNS (the luminal membrane of BBB endothelia), intestine, kidney, liver, placenta, testis, and stem cells, contributing to the absorption, distribution, and elimination of drugs and endogenous compounds (Schnepf and Zolk, 2013). Since its discovery in 1998, many drugs and endogenous substances have been identified to be transported by BCRP (Doyle et al., 1998; Lee et al., 2015). Brain penetration studies in naive, *Mdr1a/b*$^{-/-}$, *Bcrp1*$^{-/-}$, and *Mdr1a/b*$^{-/-}$*Bcrp1*$^{-/-}$ mice or rats clearly illustrated the restrictive effect of BCRP1 on brain disposition for substrate drugs, such as cancer therapeutics, dantrolene, and phytoestrogens (Enokizono et al., 2007; Schnepf and Zolk, 2013). Recent liquid chromatography–tandem mass spectrometry (LC-MS/MS)–based proteomic analyses revealed that BCRP is the most abundant transporter at human BBB

[1]Current affiliation: Pharmacokinetics and Drug Metabolism, Asia Pacific TMED, Sanofi, Shanghai, China.

https://doi.org/10.1124/dmd.116.074245.

[S]This article has supplemental material available at dmd.aspetjournals.org.

ABBREVIATIONS: ABC, ATP-binding cassette; BBB, blood-brain barrier; BCRP, breast cancer resistance protein; CNS, central nervous system; ER, efflux ratio; $K_{p,uu}$, unbound brain-to-blood (plasma) concentration ratio; LC-MS/MS, liquid chromatography–tandem mass spectrometry; MDCK, Madin-Darby canine kidney; MOI, multiplicity of infection; PCR, polymerase chain reaction; P-gp, P-glycoprotein; PS, permeability surface; WT, wild type.

and shows approximately 2-fold higher expression in human than in rodent. This is in contrast to about 2- to 3-fold lower P-gp expression at the BBB in human than in rodent (Kamiie et al., 2008; Uchida et al., 2011b; Hoshi et al., 2013). In addition, BCRP expression is up-regulated in some neurodegenerative diseases such as Alzheimer disease and amyotrophic lateral sclerosis patients (Xiong et al., 2009; Jablonski et al., 2012). These data could imply a more prominent role of BCRP in brain penetration in diseased humans compared with mice and rats.

Despite this emerging evidence, BCRP is largely overlooked in CNS drug discovery programs due to several reasons. First, BCRP and P-gp share largely overlapping substrate specificity. These transporters cooperate to limit the brain distribution of their cosubstrates and compensate for each other when the function of one is impaired. Teasing out BCRP-specific impact on drug brain penetration in intact systems is not an easy task, in part due to the limited specificity of substrates and inhibitors. In addition, utilization of mouse or rat as the most-evaluated preclinical species to examine the role of efflux transporters at the BBB in brain penetration may underestimate and reinforce the contribution of BCRP and P-gp, respectively, due to species difference in protein expression. Second, BCRP is distinct from P-gp and multidrug resistance–associated protein since it is a half-transporter that functions as a dimer or oligomer (Poguntke et al., 2010). The structural understanding of drug binding and transport by BCRP is still incomplete. The structural and physicochemical properties governing the interaction with BCRP remain largely unexplored. This complexity poses many uncertainties for project teams in relation to knowing how to walk away from this liability. Third, the predictive value of in vitro BCRP transport assays remains controversial. BCRP was reported to play a minimal role at the BBB in vivo despite mediating transport of various compounds in vitro (Zhao et al., 2009). Another study did not demonstrate a positive relationship between in vivo and in vitro BCRP activities in brain and testis penetration for eight compounds (Enokizono et al., 2008). These knowledge gaps cast doubt on the benefit of compound screening against BCRP in CNS discovery projects.

In the present study, we aimed to examine the relationship between BCRP expression and transcellular transport activity using newly constructed human and murine BCRP-expressing MDCKII cells. We have also examined species differences in mouse and human BCRP transport activities for 12 drugs. Finally, we examined the relationship between the BCRP efflux ratio (ER) and the rodent unbound brain-to-blood (plasma) concentration ratio ($K_{p,uu}$) for 25 compounds, which were BCRP substrates but not P-gp or weak P-gp substrates.

Materials and Methods

Materials. Axitinib and flavopiridol were purchased from Toronto Research Chemicals (Toronto). Dantrolene sodium salt, coumestrol, prazosin hydrochloride, and Ko143 were obtained from Sigma (St. Louis, MO). Daidzein was procured from J&K Chemical Ltd. (Shanghai, China); genistein was procured from Acros Organics (Thermo Fisher Scientific, Waltham, MA); erlotinib hydrochloride and sunitinib maleate were procured from BIONET (Cornwall, United Kingdom); dasatinib and gefitinib were procured from Nanjing Chemlin Chemicals Co., Ltd. (Nanjing, China); and imatinib tosylate and sorafenib tosylate were procured from Far Top Limited Co., Ltd. (Nanjing, China). LY335979 hydrochloride was purchased from Shanghai Haoyuan Chemexpress Co., Ltd. (Shanghai, China). Amprenavir was obtained from the GlaxoSmithKline compound library. Cell culture reagents were purchased from Invitrogen (Carlsbad, CA). All other reagents used were of bioanalytical grade or higher. For BCRP and BCRP1 quantification, signature peptide (SSLLDVLAAR) standard and corresponding stable isotope labeled ([^{13}C^{15}N]-leucine, SSLLDVL*AAR) internal standard were obtained from GL Biochem (Shanghai) Ltd. (Shanghai, China). The ProteoExtract native membrane protein extraction kit was procured from Calbiochem (Temecula, CA). The protein quantification bicinchoninic acid assay kit was purchased from Thermo Fisher Scientific. Tosylsulfonyl-phenylalanyl-chloromethyl ketone-treated trypsin from bovine pancreas was purchased from Sigma and used for protein digestion. Iodoacetamide was obtained from Sigma and dithiotrietol was purchased from Fluka (Buchs, Switzerland).

Generation of BacMam2 Virus Carrying Human BCRP and Murine Bcrp1 cDNA. ABCG2 human cDNA was amplified from brain, placenta, and testis cDNA using polymerase chain reaction (PCR) and then cloned into pCDNA3.2TOPO. The BCRP sequence was verified in-house. Abcg2 murine cDNA clone was purchased from Origene (Rockville, MD). PCR cloning of human BCRP or murine Bcrp1 cDNA into pHTBV1mcs3 vector between BamHI and XhoI sites was verified. The BacMam plasmid pHTBV-BCRP or pHTBV-Bcrp1 was transformed into DH10Bac *Escherichia coli* competent cells (Invitrogen), and a single colony from a freshly streaked selective plate was picked and inoculated into 5.0 ml of medium containing the appropriate selective antibiotic. After ~16 hour of incubation at 37°C with vigorous shaking (200 rpm), bacmid DNA was extracted. The purified BCRP or Bcrp1 bacmid DNA was transfected into Sf9 cells in 6-well dishes at 9×10^5 cells/well using Cellfectin (Invitrogen). After 3 to 4 days when the cytopathic effect (the inhibition of cell growth and lysis of cells) was evident, the culture was collected and centrifuged to pellet the cell debris. The supernatant containing the virus (P0 virus) was transferred to a sterile 15-ml screw-cap tube, and stored at 4°C in the dark. The virus stock was further amplified by infecting 200 ml of Sf9 cells (2×10^6 cells/ml) at a multiplicity of infection (MOI) ranging from 0.05 to 0.1. The P1 virus was harvested 4 days later, and titration was performed in a viral plaque assay using the BacPAK Baculovirus Rapid Titer Kit (Clontech, Palo Alto, CA). The recombinant virus was confirmed to contain the human BCRP or murine Bcrp1 gene insert by PCR using extracted virus DNA as the template and referred to as BacMam2-BCRP or BacMam2-Bcrp1.

Construction of Human BCRP- and Murine BCRP1-Expressing MDCKII Cells. Polarized MDCKII wild-type (WT) cells were obtained from The Netherlands Cancer Institute (Amsterdam). MDCKII cells were seeded at a density of 0.1 million/transwell insert in Dulbecco's modified Eagle's medium with 10% fetal bovine serum. BacMam2-BCRP or BacMam2-Bcrp1 at an appropriate MOI was administered to the apical side of the 24-well transwell inserts (Millipore Corporation, Bedford, MA) 24 hours post MDCKII cell seeding. The cells were cultured for another 48 hours before transport experiments.

Transport Studies across BacMam2-BCRP or BacMam2-Bcrp1 Cells. On the day of transport experiments, donor solutions were prepared by diluting test compounds in transport medium (Dulbecco's modified Eagle's medium supplemented with 4500 mg/l D-glucose, L-glutamine, and 25 mM HEPES but without sodium pyruvate and phenol red, pH 7.4). The receiver solution was the transport medium. The transport of the test compounds was measured in both directions [apical to basolateral (A→B) and basolateral to apical (B→A)] for 90 minutes in the absence and presence of transporter inhibitor. The transepithelial electrical resistance was measured using a Millipore Millicell-ERS System with chopstick electrodes (Millipore Corporation). Lucifer yellow was used as a paracellular marker to determine the integrity of MDCKII monolayers and was measured by a SpectraMax Gemini Cytofluorimeter (Molecular Devices, Sunnyvale, CA) set to an excitation wavelength of 430 nm and emission wavelength of 540 nm. The exact permeability (P_{exact}, nm/s) and mass balance (MB) percentage for test compound across MDCKII monolayers were determined using the eqs. 1 & 2, as follows:

$$P_{exact} = -\left(\frac{V_D V_R}{(V_D + V_R)At}\right)\ln\left\{1 - \frac{(V_D + V_R)C_R(t)}{[V_D C_D(t) + V_R C_R(t)]}\right\} \times 10^7 \quad (1)$$

$$MB(\%) = \frac{V_D C_D(t) + V_R C_R(t)}{V_D C_D(t0)} \times 100 \quad (2)$$

where V_D and V_R are the donor and receiver well volumes (in ml), respectively; A is the membrane surface area (in cm^2); t is the transport time (in seconds); $C_R(t)$ and $C_D(t)$ are the measured mass spectrometric response or concentration of the test compound in the receiver and donor wells at time t (90 minutes), respectively; and $C_D(t0)$ is the measured mass spectrometric response or concentration of the

test compound in the initial donor solution at time 0. Equation 1 was also used to determine the membrane permeability of lucifer yellow.

The ER is defined as the permeability ratio of the basolateral-to-apical direction to the apical-to-basolateral direction. The corrected ER is the ratio of ER in the absence of inhibitor to the presence of inhibitor completely abolishing transporter activity. This is introduced to take into account any involvement of endogenous transporters in MDCKII-WT cells in transcellular transport of test compounds.

Quantification of Test Compounds in Transport Samples by LC-MS/MS. Quantification of drugs in MDCKII transport samples was performed using the ACQUITY UPLC system (Waters, Milford, MA) coupled with the 4000 Q-Trap or API 5000 triple-quadrupole mass spectrometer (AB Sciex, Foster City, CA). The samples were processed by deproteination with the same volume of acetonitrile containing an appropriate internal standard. The chromatographic separation was achieved on a Waters ACQUITY UPLC BEH C_{18} or UPLC HSS T3 (50 × 2.1 mm, 1.7 μm) analytic column at 40°C, using a gradient of aqueous (solvent A: 1 mM ammonia acetate in water or 0.1% formic acid in water) and organic [solvent B: CH3CN-CH3OH with or without 0.1% formic acid (4:1, v/v)] mobile phase at a flow rate of 600 μl/min. The run time for each compound was 2.0 minutes. The key chromatographic and mass spectrometric settings were optimized to yield the best sensitivity for each test compound and are detailed in Supplemental Table 1.

Protein Quantification of Human BCRP and Murine BCRP1 by LC–MS/MS. Protein quantification of human BCRP in BacMam2-BCRP–transduced or murine BCRP1 in BacMam2-Bcrp1–transduced MDCKII membrane extracts was conducted by mass spectrometry–based targeted proteomics using validated LC-MS/MS methods. Briefly, the cells were harvested from semipermeable membranes in the transwell inserts using extraction buffer I in the ProteoExtract membrane extraction kit (Calbiochem). Total membrane proteins were isolated and digested using a previously outlined procedure (Kamiie et al., 2008; Uchida et al., 2013).

The chromatographic and spectrometric conditions for protein quantification of BCRP and BCRP1 are described subsequently. Trypsin digest (8 μl) was injected onto the column (ACQUITY UPLC HSS T3, 2.1 × 100 mm, 1.8 μm). A mobile phase consisting of water containing 0.2% acetic acid (A) and acetonitrile-methanol (1:1, v/v) containing 0.2% acetic acid (B) was employed. A flow rate of 0.5 ml/min was used with elution starting at 20% B for 0.2 minutes, followed by a linear gradient increasing to 60% B (0.2–4.5 minutes). This was followed by another steep linear gradient increasing to 95% B (4.5–4.55 minutes) and then eluting the column with 95% mobile phase B for 0.65 minutes, and re-equilibrating it at 20% B for 1.25 minutes. The MS/MS analysis of BCRP and BCRP1 was performed by monitoring the signature peptide (522.5–644.7) and the internal standard (526.8–651.7) using an optimized cone voltage and collision energy. Representative LC-MS/MS chromatograms and calibration curves of the surrogate peptide are shown in Supplemental Fig. 1.

The accuracy and precision of the assay were >80% and <20%, respectively. BCRP and BCRP1 protein expression data (picomoles per milligram) were expressed relative to the total protein content of the isolated membrane, as determined by the Pierce BCA Protein Assay Kit (Pierce, Rockford, IL). All samples were digested and measured in duplicate.

Relationship between the ER and Efflux Activity. The relationship between the ER and the efflux activity (PS_{efflux}) for BCRP across MDCKII monolayers was adapted from a three-compartment model (apical, cellular, and basolateral) described previously (Kalvass and Pollack, 2007):

$$PS_{efflux} = 2PS(ER - 1) \quad (3)$$

where PS_{efflux} is the BCRP-mediated efflux activity; PS is the passive permeability-surface area product; and ER is the permeability ratio of the basolateral-to-apical direction to the apical-to-basolateral direction. The corrected ER was also used herein to take into account any influence introduced by endogenous transporters in MDCKII-WT cells. Based on eq. 3, the PS_{efflux} value is quantitatively proportional to ER-1 multiplied by the passive permeability.

Dantrolene is a specific BCRP substrate and was used as a reference compound in each in vitro experiment. Under the condition of the linear relationship between BCRP expression and in vitro or in vivo transcellular transport activity, the following equation is derived:

$$\frac{PS_{\text{in vitro, test compound}}}{PS_{\text{in vivo, test compound}}} = \frac{PS_{\text{in vitro, Dan}}}{PS_{\text{in vivo, Dan}}} \quad (4)$$

Substituting eq. 3 into eq. 4 and rearranging yield the following equation:

$$\frac{ER_{\text{in vitro, test compound}} - 1}{ER_{\text{in vitro, Dan}} - 1} = \frac{ER_{\text{in vivo, test compound}} - 1}{ER_{\text{in vivo, Dan}} - 1} \quad (5)$$

where $ER_{\text{in vivo}}$ is defined as the brain-to-plasma (blood) ratio in Bcrp-deficient animals divided by the brain-to-blood (plasma) ratio in Bcrp-competent animals at

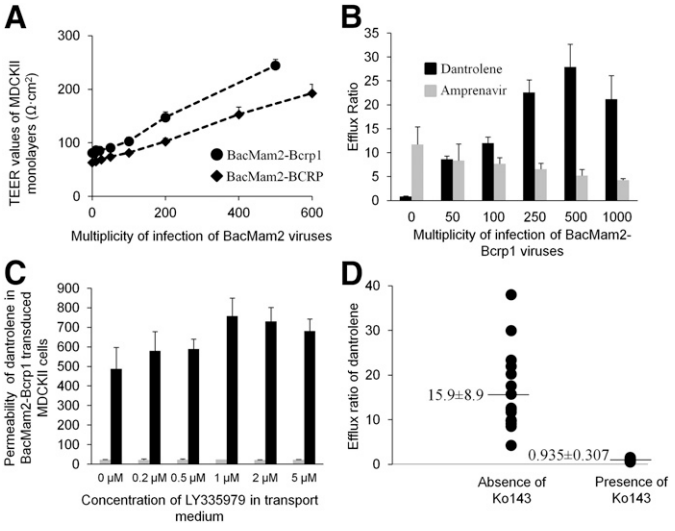

Fig. 1. Construction of MDCKII monolayers expressing human BCRP and murine BCRP1. (A) Transepithelial electrical resistance (TEER) values of MDCKII-WT monolayers after transduction of varying MOI of BacMam2-Bcrp1 (murine) and BacMam2-BCRP (human) viruses (n = 12). (B) ERs of dantrolene and amprenavir (n = 3, donor concentration 1 μM) across MDCKII-WT monolayers transduced with varying MOIs of BacMam2-Bcrp1 viruses. (C) Effect of different concentrations of P-gp–specific inhibitor LY335979 on apical-to-basolateral (gray bar) and basolateral-to-apical (black bar) permeability of dantrolene (n = 3, donor concentration 1 μM) across BacMam2-Bcrp1 transduced MDCKII-WT monolayers. (D) ER of dantrolene (donor concentration 3 μM) from 16 consecutive transport experiments across BacMam2-BCRP transduced MDCKII-WT monolayers in the absence or presence of 0.2 μM of Ko143; mean ± S.D. is indicated near the horizontal solid line.

TABLE 1

Protein expression of BCRP in membrane extracts and corrected ERs of dantrolene, coumestrol, daidzein, and genistein across MDCKII monolayers transduced with varying titers of BacMam2-BCRP viruses

Protein Level of BCRP[a]	Corrected ER[b]			
	Dantrolene	Coumestrol	Daidzein	Genistein
fmol/μg·protein				
0	0.63 ± 0.22	1.09 ± 0.58	0.80 ± 0.10	0.52[c]
3.47	1.09 ± 0.15	3.00[c]	1.86 ± 0.36	1.32 ± 0.32
13.4	2.62 ± 0.31	3.99 ± 1.17	5.95 ± 0.61	1.59 ± 0.75
34.4	3.56 ± 0.77	7.67 ± 1.86	10.9 ± 3.0	7.21 ± 3.86
60.6	6.39 ± 1.59	10.7 ± 2.4	10.5 ± 6.3	8.09[c]
50.1[d]	7.24 ± 0.75	18.6 ± 4.0	18.4 ± 2.3	10.0 ± 2.2

[a]Protein levels are the mean value of duplicate measurements.
[b]Data are presented as the mean ± S.D. from three individual transwell assays unless otherwise indicated.
[c]The corrected ER was calculated from the permeability with at least one averaged from two individual transwell assays.
[d]The MDCKII cells were transduced with the highest titers of BacMam2-BCRP. The protein level of BCRP from the membrane extract was likely underestimated since these cells had the highest mRNA level (assayed by quantitative polymerase chain reaction) and BCRP efflux activity. These cells also had the highest protein level of BCRP when assayed by the LC-MS/MS technique with another different surrogate peptide (ATEIIEPSK).

steady state. The $K_{p,uu}$ value of a discovery compound can be described by the reciprocal of $ER_{in\ vivo}$ value as follows (Uchida et al., 2011a):

$$K_{p,uu} = \frac{1}{ER_{in\ vivo,\ test\ compound}} \quad (6)$$

Statistical Analysis. The permeability and ERs are presented as the mean ± S.D. of technical or experimental replicates. The protein levels are the mean values of duplicate measurements. Linear regression analysis was performed with Microsoft Excel 2007. In all cases, $P < 0.05$ was considered to be statistically significant.

Results

Construction of MDCKII Monolayers Expressing BCRP or BCRP1. BacMam2 viruses carrying BCRP or Bcrp1 cDNA in Dulbecco's modified Eagle's medium were dosed into the apical side of the transwell inserts at a designated MOI. Transport studies were carried out 2 days after transduction of BacMam2. The transepithelial electrical resistance values of MDCKII monolayers were elevated after BacMam2 virus transduction. The extent of increase in the transepithelial electrical resistance values correlated positively with the MOI of BacMam2 (Fig. 1A). Low permeability of paracellular marker Lucifer yellow (typically, <20 nm/s) confirmed the tightness of MDCKII-Bcrp1 or MDCKII-BCRP monolayers. MDCKII-WT cells expressed endogenous canine P-gp, the transport activity of which was probed by amprenavir, a P-gp–specific substrate. The ER of amprenavir was reduced along with increasing transport of dantrolene, a specific probe substrate of BCRP1 (Fig. 1B). This was consistent with reverse correlation of canine P-gp and BCRP mRNA levels in BacMam2-BCRP–transduced MDCKII cells (data not shown). Inclusion of 1 μM of P-gp–specific inhibitor LY335979 in transport medium completely inhibited endogenous P-gp activity (Shepard et al., 2003), with no effect on BCRP1 activity in MDCKII cells (Fig. 1C). Interbatch variability in BCRP transport activity was notable (Fig. 1D). The ER of dantrolene was 15.9 ± 8.9 in 16 consecutive experiments with a coefficient of variation of 56% in MDCKII-BCRP cells. The ER of dantrolene collapsed to around unity (0.935 ± 0.307) in the presence of 0.2 μM of BCRP-specific inhibitor Ko143 in transport medium (Allen et al., 2002).

Correlation between BCRP Membrane Protein Concentration and Transcellular Transport Activity across MDCKII Monolayers. The BCRP and BCRP1 protein levels in membrane extracts of MDCKII cells transduced by BacMam2 viruses were quantified by a validated LC-MS/MS method. While the multiple surrogate peptides for BCRP and BCRP1 were observed to have different absolute quantitative values, these correlated strongly (data not shown; R^2 typically greater than 0.9). The difference could be the result of differential digestion efficiency of signature peptides, unexpected post-translational modifications of signature peptides, or inaccurate quantification of synthetic signature peptides. We report herein, protein expression levels measured by a surrogate peptide consistently providing the highest protein quantification results, which may more accurately represent the true protein abundance, as reported previously (Balogh et al., 2013; Peng et al., 2015).

MDCKII cells with different levels of protein expression of BCRP or BCRP1 were generated by titrating the MOI of BacMam2-BCRP or BacMam2-Bcrp1 virus in transwell apical compartments. A linear correlation between mRNA level and protein expression for BCRP was observed for the initial five MOI investigated. Higher BacMam2-BCRP or BacMam2-Bcrp1 virus load led to reduction in mRNA level (data not shown). This might be due to interference in the transcription

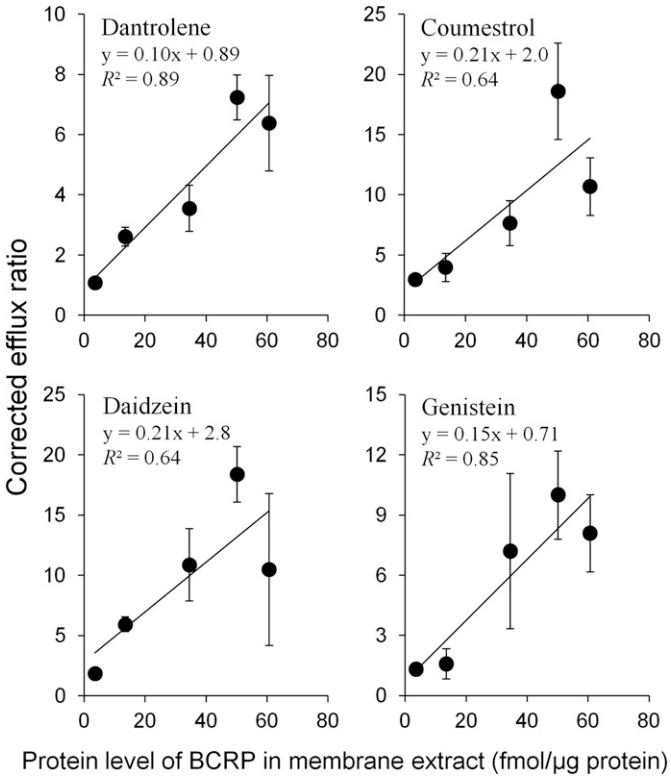

Fig. 2. Correlation of BCRP expression level in membrane extracts of BCRP-expressing MDCKII cells with in vitro corrected ERs of dantrolene, coumestrol, daidzein, and genistein. ERs are presented as mean ± S.D. from three individual transwell assays. Protein levels are the mean value of duplicate measurements.

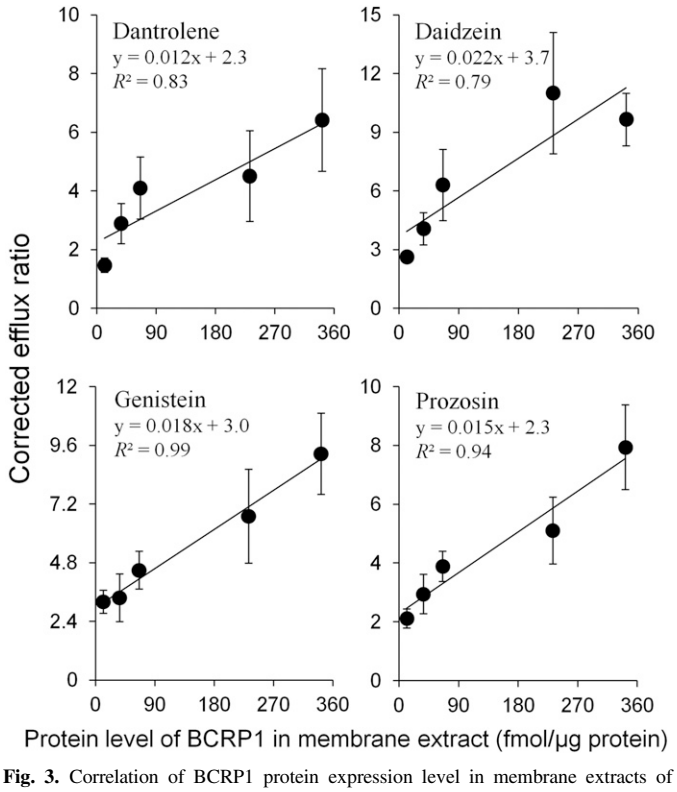

Fig. 3. Correlation of BCRP1 protein expression level in membrane extracts of BCRP1-expressing MDCKII cells with in vitro corrected ERs of dantrolene, daidzein, genistein, and prosozin. ERs are presented as mean ± S.D. from three individual transwell assays. Protein levels are the mean value of duplicate measurements.

TABLE 2

Protein expression of BCRP1 in membrane extracts and corrected ERs of dantrolene, daidzein, genistein, and prazosin across MDCKII monolayers transduced with varying titers of BacMam2-Bcrp1 viruses

Protein Level of BCRP1[a]	Corrected ER[b]			
	Dantrolene	Daidzein	Genistein	Prazosin[c]
fmol/μg·protein				
0	0.79 ± 0.27	1.07 ± 0.23	0.62 ± 0.17	0.71 ± 0.20
11.5	1.47 ± 0.24	2.62 ± 0.20	3.21 ± 0.47	2.12 ± 0.32
36.5	2.89 ± 0.69	4.07 ± 0.82	3.37 ± 0.97	2.95 ± 0.67
65.7	4.10 ± 1.06	6.31 ± 1.82	4.50 ± 0.77	3.89 ± 0.51
232	4.51 ± 1.54	11.0 ± 3.1	6.71 ± 1.92	5.11 ± 1.14
342	6.42 ± 1.75	9.66 ± 1.34	9.26 ± 1.66	7.94 ± 1.44

[a]Protein levels are the mean value of duplicate measurements.
[b]Data are presented as the mean ± S.D. from three individual transwell assays.
[c]One micromolar of LY335979 was included in the transport medium of prazosin.

and translation pathway of BCRP by high BacMam2 virus load, and therefore these specific data were not included in the following correlation analysis.

Dantrolene, coumestrol, daidzein, and genistein are BCRP-specific substrates (Enokizono et al., 2007; Fuchs et al., 2014). Transport of these four compounds across MDCKII monolayers with different levels of BCRP expression was examined (Table 1; Supplemental Table 2). The ERs of coumestrol, daidzein, and genistein were collapsed to 0.5 or below in the presence of BCRP inhibitor Ko143, indicating their transcellular transport across MDCKII monolayers was impacted by endogenous canine transporters. Thus, the corrected ER was used herein to represent BCRP-mediated transport activity. Three micromolar donor concentrations were used in this investigation. A plot of the human BCRP levels in membrane extracts versus in vitro corrected ERs in BacMam2-BCRP–transduced MDCKII cells showed a significant correlation for dantrolene ($R^2 = 0.89$, $P < 0.05$) and genistein ($R^2 = 0.85$, $P < 0.05$) and a moderate correlation for coumestrol ($R^2 = 0.64$, $P = 0.1$) and daidzein ($R^2 = 0.64$, $P = 0.1$) (Fig. 2).

We also investigated the relationship between BCRP1 protein expression levels in membrane extract versus in vitro corrected ERs in BacMam2-Bcrp1–transduced MDCKII cells. A strong linear correlation between protein level and in vitro corrected ER was observed for dantrolene ($R^2 = 0.83$, $P < 0.05$), daidzein ($R^2 = 0.79$, $P < 0.05$), genistein ($R^2 = 0.99$, $P < 0.01$), and prazosin ($R^2 = 0.94$, $P < 0.01$) (Fig. 3; Table 2; Supplemental Table 3). The P-gp–specific inhibitor LY335979 was included in the transport medium with prazosin, a known P-gp and BCRP cosubstrate (Zhou et al., 2009). According to eq. 3, these results indicated a linear correlation between expression level and transcellular transport activity for BCRP (PS_{efflux}) within the ERs investigated.

Correlation between BCRP and BCRP1 ERs across MDCKII Monolayers. The in vitro BCRP1 and BCRP ERs were assessed using a set of drugs including P-gp and BCRP cosubstrates across MDCKII monolayers. Endogenous canine P-gp activity was inhibited by including LY335979 (1 μM) in transport medium. To avoid data differences due to any interbatch variation in BCRP expression, the 12 drugs were evaluated in a single experiment. One micromolar donor concentration was used for all drugs. All of the selected drugs were identified to be murine and human BCRP substrates. The ERs for these drugs were greater than 2 and collapsed to around or below unity in the presence of the BCRP-specific inhibitor Ko143 (Tables 3 and 4). When the impact of BCRP on directional transport was ranked across all tested drugs, considerable overlap between human and mouse was observed. The corrected ERs of BCRP1 and BCRP were within 2-fold for all drugs except flavopiridol, which had 2.2-fold higher efflux in human (Fig. 4).

TABLE 3

Permeability and ERs of drugs across MDCKII monolayers transduced with BacMam2-BCRP viruses

Permeability across MDCKII-BCRP was determined with 1 μM of donor concentration and 90 minutes of transport time. One micromolar of LY335979 was included in the transport medium. Data are presented as the mean ± S.D. from three individual transwell assays.

Drug	Transport Medium without Ko143 and with 1 μM of LY335979					Transport Medium with 0.2 μM of Ko143 and 1 μM of LY335979					Corrected ER
	$P_{A\to B}$	MB (A→B)	$P_{B\to A}$	MB (B→A)	ER	$P_{A\to B}$	MB (A→B)	$P_{B\to A}$	MB (B→A)	ER	
	nm/s	*%*	*nm/s*	*%*		*nm/s*	*%*	*nm/s*	*%*		
Dantrolene	54.0 ± 4.9	92.6	484 ± 179	95.7	8.98 ± 3.42	453 ± 24	95.0	228 ± 4	91.5	0.503 ± 0.028	17.8 ± 6.9
Coumestrol	29.3 ± 1.0	85.9	287 ± 36	97.6	9.80 ± 1.29	143 ± 25	47.7	49.4 ± 2.5	88.7	0.345 ± 0.063	28.4 ± 6.4
Daidzein	26.9 ± 6.8	95.9	745 ± 155	96.4	27.7 ± 9.0	224 ± 19	78.9	147 ± 25	96.6	0.657 ± 0.125	42.1 ± 15.9
Axitinib	114 ± 4	92.6	353 ± 9	91.3	3.10 ± 0.14	324 ± 26	87.3	224 ± 25	103	0.691 ± 0.095	4.49 ± 0.65
Dasatinib	8.94 ± 0.51	110	268 ± 16	98.8	29.9 ± 2.5	110 ± 10	92.3	71.2 ± 5.1	113	0.646 ± 0.077	46.4 ± 6.7
Erlotinib	53.3 ± 8.5	117	423 ± 89	117	7.93 ± 2.08	304 ± 22	97.6	228 ± 39	100	0.749 ± 0.139	10.6 ± 3.4
Flavopiridol	20.3 ± 1.8	103	610 ± 43	107	30.1 ± 3.4	274 ± 6	94.2	176 ± 24	130	0.642 ± 0.090	46.9 ± 8.4
Gefitinib	19.4 ± 1.2	90.9	471 ± 36	87.7	24.3 ± 2.4	177 ± 18	71.8	106 ± 6	99.1	0.596 ± 0.067	40.8 ± 6.1
Imatinib	22.8 ± 2.3	73.6	301 ± 30	74.8	13.2 ± 1.9	201 ± 42	72.0	113 ± 10	79.4	0.565 ± 0.130	23.4 ± 6.3
Prazosin	28.6 ± 3.5	106	395 ± 13	94.4	13.8 ± 1.8	310 ± 9	104	212 ± 62	98.3	0.684 ± 0.200	20.2 ± 6.4
Sorafenib	17.7 ± 5.6	43.8	53.8 ± 4.3	81.3	3.05 ± 1.00	20.3 ± 3.5	42.6	3.66 ± 0.23	79.2	0.180 ± 0.033	16.9 ± 6.3
Sunitinib	34.8 ± 7.1	88.0	418 ± 18	82.1	12.0 ± 2.5	158 ± 10	63.8	84.9 ± 11.7	76.3	0.536 ± 0.082	22.4 ± 5.8

MB, mass balance; MB (A→B), apical-to-basolateral mass balance in percentage; MB (B→A), basolateral-to-apical mass balance in percentage; $P_{A\to B}$, apical-to-basolateral permeability; $P_{B\to A}$, basolateral-to-apical permeability.

TABLE 4

Permeability and ERs of drugs across MDCKII monolayers transduced with BacMam2-Bcrp1 viruses

Permeability across MDCKII-Bcrp1 was determined with 1 μM of donor concentration and 90 minutes of transport time. One micromolar of LY335979 was included in the transport medium. Data are presented as the mean ± S.D. from three individual transwell assays.

Drug	Transport Medium without Ko143 and with 1 μM of LY335979					Transport Medium with 0.2 μM of Ko143 and 1 μM of LY335979					Corrected ER
	$P_{A\rightarrow B}$	MB (A→B)	$P_{B\rightarrow A}$	MB (B→A)	ER	$P_{A\rightarrow B}$	MB (A→B)	$P_{B\rightarrow A}$	MB (B→A)	ER	
	nm/s	%	*nm/s*	%		*nm/s*	%	*nm/s*	%		
Dantrolene	32.9 ± 5.4	103	822 ± 85	112	25.0 ± 4.9	387 ± 12	102	361 ± 52	94.9	0.931 ± 0.137	26.9 ± 6.5
Coumestrol	24.2 ± 1.9	95.8	407 ± 89	117	16.8 ± 3.9	156 ± 8	47.5	45.9 ± 6.6	108	0.295 ± 0.045	57.0 ± 15.8
Daidzein	20.4 ± 2.5	100	673 ± 86	97.4	33.0 ± 5.8	246 ± 19	68.6	151 ± 18	92.5	0.614 ± 0.088	53.8 ± 12.2
Axitinib	100 ± 8	103	294 ± 43	104	2.94 ± 0.49	336 ± 21	80.7	227 ± 29	87.3	0.678 ± 0.096	4.34 ± 0.95
Dasatinib	10.0 ± 0.4	99.3	218 ± 34	95.0	21.8 ± 3.5	157 ± 11	80.1	98.9 ± 2.6	91.8	0.631 ± 0.049	34.5 ± 6.1
Erlotinib	65.4 ± 3.9	92.7	842 ± 125	93.2	12.9 ± 2.1	368 ± 18	106	332 ± 13	93.3	0.902 ± 0.056	14.3 ± 2.4
Flavopiridol	23.0 ± 0.5	95.9	388 ± 34	96.6	16.9 ± 1.6	319 ± 10	96.5	252 ± 23	97.7	0.789 ± 0.076	21.4 ± 2.9
Gefitinib	18.4 ± 2.5	95.4	309 ± 57	93.9	16.8 ± 3.9	206 ± 4	80.2	92.0 ± 13.8	102	0.448 ± 0.068	37.5 ± 10.3
Imatinib	31.9 ± 3.7	97.5	644 ± 42	96.6	20.2 ± 2.7	277 ± 15	101	187 ± 17	99.2	0.674 ± 0.071	29.9 ± 5.1
Prazosin	27.5 ± 3.5	99.0	596 ± 53	96.7	21.6 ± 3.4	414 ± 11	110	508 ± 27	100	1.23 ± 0.07	17.6 ± 2.9
Sorafenib	14.2 ± 4.1	46.3	65.3 ± 8.2	65.3	4.60 ± 1.45	47.2 ± 3.3	29.9	24.9 ± 2.9	77.3	0.528 ± 0.071	8.70 ± 2.98
Sunitinib	30.7 ± 4.0	87.3	418 ± 97	87.3	13.6 ± 3.6	156 ± 6	66.4	106 ± 34.7	77.2	0.678 ± 0.224	20.0 ± 8.5

MB, mass balance; MB (A→B), apical-to-basolateral mass balance in percentage; MB (B→A), basolateral-to-apical mass balance in percentage; $P_{A\rightarrow B}$, apical-to-basolateral permeability; $P_{B\rightarrow A}$, basolateral-to-apical permeability.

Discussion

Screening for BCRP substrates in CNS drug discovery is mainly issue driven and this typically takes place when a discovery compound with high passive permeability has a low $K_{p,uu}$ value and is not a strong P-gp substrate (Di et al., 2013; Poirier et al., 2014). A challenge facing project teams is how to contextualize the in vitro MDCKII-BCRP transport data. To predict transporter-mediated disposition at the BBB, physiologically based pharmacokinetic approaches use in vitro data from over-expressing cell lines and scale these to the in vivo data by correcting the differences in transporter protein expression via in vitro/in vivo extrapolation. This approach requires making two assumptions: 1) passive permeability is similar across epithelial (MDCK) and endothelial (BBB) membranes; and 2) there is a linear correlation between expression and activity of the transporter protein (Kumar et al., 2015). Available evidence supports the hypothesis that there is no substantial difference in passive permeability across epithelial and endothelial membranes (Uchida et al., 2011a; Liu et al., 2014). The current study aims to examine the validity of the second assumption for BCRP, using MDCKII-BCRP and MDCKII-Bcrp1 monolayers. Our data demonstrate a linear correlation between BCRP membrane protein expression and BCRP-mediated transcellular transport activity across MDCKII monolayers, within the ERs investigated. This implies that it is feasible to predict BCRP-mediated in vivo impact on brain penetration using a BCRP-expressing MDCKII transwell system. This was previously exemplified by P-gp substrates that showed transcellular transport activity was proportional to the transporter expression levels (Tachibana et al., 2010). Successful reconstruction of in vivo brain distribution of P-gp substrates has been based on the BBB transporter protein concentration, in vitro intrinsic transport activity, and in vitro transporter expression in mice and monkey (Uchida et al., 2011a, 2014).

Dantrolene is a specific BCRP substrate with well-characterized BBB transport profiles in preclinical species. We use this reference drug as an indicator of BCRP competency in the transwell system. A review of the literature showed that the in vivo brain penetration ERs of dantrolene in *Bcrp1*$^{-/-}$ to WT mice and rats were 6.30 and 3.30 at steady state, respectively, and the mean Bcrp expressions at the mouse, rat, and human BBBs were 3.37, 4.15, and 7.15 fmol/μg·protein, respectively (Table 5). By averaging the Bcrp expression and in vivo brain penetration ERs in mice and rats and assuming no species differences in BCRP transport activity, we predicted the human $ER_{in\ vivo,\ Dan}$ to be 9.1 and the unbound brain-to-plasma concentration ratio to be 0.11 (Table 5). The predicted human BCRP $ER_{in\ vivo}$ of dantrolene is useful to contextualize the BCRP in vitro transport data for discovery compounds. A $K_{p,uu}$ value greater than 0.3 is typically used as a starting point of acceptable brain penetration in CNS drug discovery programs. Based on eq. 5 and 6, this would require $(ER_{in\ vitro,\ test\ compound} - 1)/(ER_{in\ vitro,\ Dan} - 1) < (1/0.3 - 1)/(9.1 - 1) = 0.29$ in MDCKII-BCRP transport studies. Conversely, $(ER_{in\ vitro,\ test\ compound} - 1)/(ER_{in\ vitro,\ Dan} - 1) > 0.29$ would predict $K_{p,uu}$ values smaller than 0.3 and raise a red flag for BCRP-mediated compromise in brain penetration at the human BBB. Verification of the strength of our predictions requires the clinical ER of dantrolene. This will now be possible because the positron emission tomography BCRP probe [^{13}N]dantrolene has been successfully synthesized (Kumata et al., 2012).

To verify this contextualization approach, we applied this method to 22 proprietary discovery compounds and three phytoestrogens including

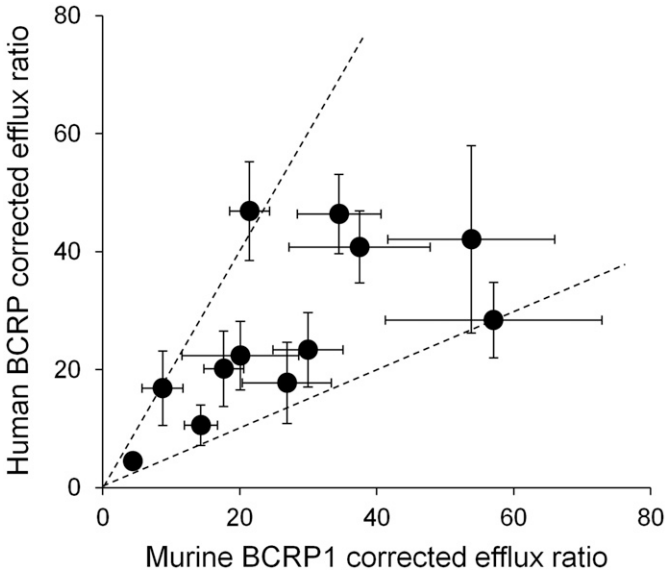

Fig. 4. Correlation of corrected ERs in transwell assays using MDCKII-Bcrp1 and MDCKII-BCRP monolayers for 12 drugs. The *y*-axis is the human BCRP-corrected ER and the *x*-axis is the murine BCRP1-corrected ER. Data are shown as mean ± S.D. (n = 3). Dashed lines are the line of 2-fold deviation from unity.

TABLE 5

Prediction of the in vivo BCRP ER of dantrolene in human based on the in vivo BCRP ER of dantrolene in preclinical species and BCRP expression at BBB

Species (Strain)	BCRP Expression at BBB	$ER_{in\ vivo}$ of Dantrolene	Predicted $K_{p,uu}$[a]	Reference
	fmol/μg·protein			
Mouse (Friend virus B)	3.53, 3.21 (mean 3.37)	6.30	0.16	Enokizono et al. (2008); Uchida et al. (2013);Agarwal et al. (2012)
Rat (Sprague Dawley)	4.15	3.30	0.30	Hoshi et al. (2013); Fuchs et al. (2014)
Human	6.15, 8.14 (mean 7.15)	9.1 (predicted)[b]	0.10	Shawahna et al. (2011); Uchida et al. (2011b)

[a]The $K_{p,uu}$ value was predicted by the reciprocal of the $ER_{in\ vivo}$ value (eq. 6).
[b]The human $ER_{in\ vivo}$ value of dantrolene was predicted by (mean $ER_{in\ vivo}$ of dantrolene in mouse and rat -1) ÷ ratio of mean BCRP expression at mouse and rat to human BBB + 1. The BCRP transport capacity was assumed to be the same in human as mouse and rat.

coumestrol, daidzein, and genistein, which are BCRP substrates but not P-gp or weak P-gp substrates (Supplemental Table 4). We observed good correlation of restricted brain penetration with benchmarked $ER_{in\ vivo}$ values in rodents (Fig. 5). Compromised brain penetration ($K_{p,uu} < 0.3$) is correctly predicted when $(ER_{in\ vitro,\ test\ compound} - 1)/(ER_{in\ vitro,\ Dan} - 1)$ is greater than 0.6 (quadrant I, where 0.6 is derived from the mean $ER_{in\ vivo}$ of dantrolene in rat and mouse). Some compounds show greater restriction in brain penetration than expected (quadrant IV), likely due to additional BBB efflux mechanisms or species differences in BCRP or P-gp transport. In our experience, it is not unusual for a compound to have limited brain penetration (e.g., $K_{p,uu} < 0.3$), even though it is not a P-gp or BCRP substrate and has high passive permeability. It is possible that members of the multidrug resistance–associated protein family of transporters are involved, or some other yet-to-be-identified efflux pathways. This highlights the gap in our understanding of the very intricate BBB. Empirically, an ER of BCRP greater than 5 was used as a red flag in brain penetration impairment. However, this empirical approach does not consider interbatch BCRP expression variability and may only be applied in our laboratory. The proposed contextualization approach has been improved by addressing this issue and may be transferable to other laboratories.

On a simpler scale, we are able to manipulate the in vitro system to minimize impact of other transporters since the endogenous canine transporters expressed on MDCKII cells may confound the transport data of P-gp and BCRP cosubstrates. MDCKII-WT cells express canine P-gp but not BCRP. In addition, endogenous P-gp expression can be impacted by BacMam virus load (Liu et al., 2015). In previous studies, the BCRP-expressing in vitro transwell system was not found to be predictive of in vivo transport activity (Enokizono et al., 2008; Zhao et al., 2009), likely because P-gp/BCRP cosubstrates were included and the activity of endogenous P-gp was ignored. In this study, inclusion of P-gp–specific inhibitor LY335979 in transport medium inhibited endogenous P-gp activity. Quantitative proteomics combined with transport studies in this relatively pure BCRP-functioning in vitro system may be a very useful method to predict the fraction of drug transported by BCRP in vivo across the BBB. This parameter is critical when predicting the $K_{p,uu}$ value of a drug and the significance of transporters in determining brain penetration of a drug (Prasad and Unadkat, 2015). In theory, the additive effect of P-gp and Bcrp on the brain-to-plasma ratio for cosubstrates can be reconstructed by their respective contribution to the net efflux at the BBB (Kodaira et al., 2010).

The mouse BCRP1 and human BCRP amino acid sequences are 81% identical and 86% homologous, with very high homology in the ATP binding region (Doyle and Ross, 2003). Despite broad use of Bcrp1 knockout mice in exploring the effect of this transporter on drug disposition, little is known about differences in the kinetics of BCRP-mediated drug transport between human and mouse. Use of newly introduced BCRP-expressing MDCKII monolayers without endogenous canine P-gp activity allows us to examine species differences in murine and human BCRP-mediated transcellular transport. To control interbatch variability in BCRP expression, 12 drugs were evaluated simultaneously in a single experiment. Good concordance of murine and human BCRP ERs across MDCKII monolayers was observed. A further comparative study with a range of chemotypes using these systems is required. Meaningful comparison can only be obtained by close monitoring of BCRP expression among different batches of MDCKII cells.

In summary, we have constructed human BCRP- and murine BCRP1-expressing MDCKII cells by BacMam2 virus transduction. Inclusion of

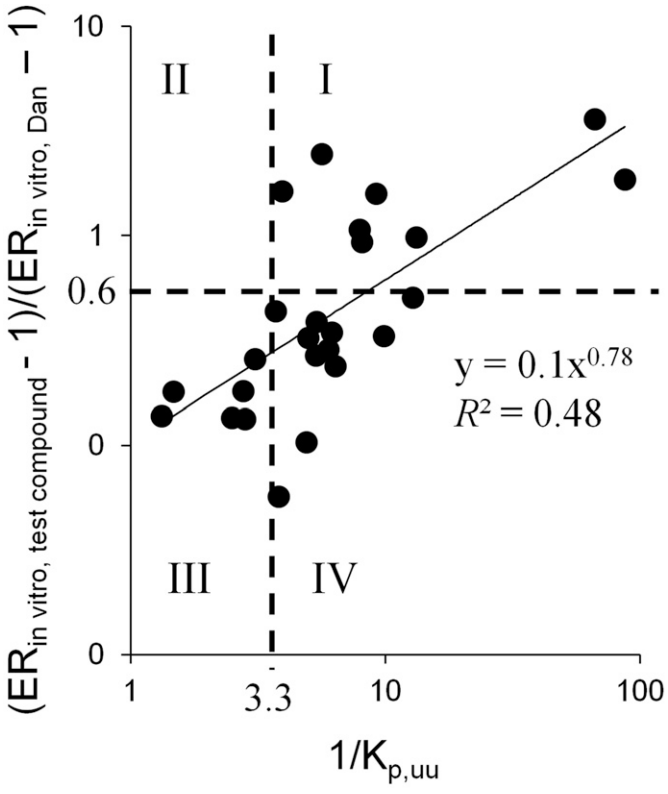

Fig. 5. Relationship between BCRP ERs and rat/mouse $K_{p,uu}$ for coumestrol, daidzein, genistein, and 22 proprietary discovery compounds. All compounds are BCRP substrates with ER > 2 across MDCKII-BCRP monolayers and ER < 1.8 or apical-to-basolateral permeability ratios in the presence to absence the P-gp inhibitor GF120918 (2 micromolar) < 1.8 across MDCKII-MDR1 monolayers. Proprietary discovery compounds have passive permeability > 250 nm/s except for two compounds, which have passive permeability = 71 nm/s. Compromised brain penetration ($K_{p,uu} < 0.3$) is predicted when $(ER_{in\ vitro,\ test\ compound} - 1)/(ER_{in\ vitro,\ Dan} - 1) > 0.6$ (eqs. 5 and 6; Table 5). Mean in vivo ER of 4.8 in rat and mouse was used. Quandrant I: $K_{p,uu} < 0.3$ and $(ER_{in\ vitro,\ test\ compound} - 1)/(ER_{in\ vitro,\ Dan} - 1) > 0.6$; quadrant II: $K_{p,uu} > 0.3$ and $(ER_{in\ vitro,\ test\ compound} - 1)/(ER_{in\ vitro,\ Dan} - 1) > 0.6$; quadrant III: $K_{p,uu} > 0.3$ and $(ER_{in\ vitro,\ test\ compound} - 1)/(ER_{in\ vitro,\ Dan} - 1) < 0.6$; quadrant IV: $K_{p,uu} < 0.3$ and $(ER_{in\ vitro,\ test\ compound} - 1)/(ER_{in\ vitro,\ Dan} - 1) < 0.6$.

P-gp–specific inhibitor LY335979 in the test system allowed us to create a relatively clean system to investigate BCRP-mediated transcellular transport across MDCKII monolayers. A linear correlation of membrane protein expression levels with transcellular transport activity for BCRP was observed within the ERs investigated. We proposed an approach to contextualize in vitro transport data of discovery compounds by benchmarking the in vitro transport data of the reference drug dantrolene and taking into account interbatch variation in BCRP expression. This approach correctly predicted impaired brain penetration for compounds, which are BCRP substrates but not P-gp or weak P-gp substrates.

Acknowledgments

The authors acknowledge Fei Wang and Dan Li for bioanalytical support. The authors also thank Sijie Lu, Xinyan Lu, and Yang Li for providing technical help on transport experiments. Finally, the authors appreciate Maciej Zamek-Gliszczynski and Joseph Polli for scientific input and helpful discussions.

Authorship Contributions

Participated in research design: Liu, Sahi, Summerfield, Dong.

Conducted experiments: Liu, Huang, Li, Sun, Gao.

Contributed new reagents or analytic tools: Chen.

Performed data analysis: Liu, Huang, Li, Y.-Y. Zhang.

Wrote or contributed to the writing of the manuscript: Liu, Fu, Y.-Y. Zhang, W. Zhang, Sahi, Summerfield, Dong.

References

Agarwal S, Uchida Y, Mittapalli RK, Sane R, Terasaki T, and Elmquist WF (2012) Quantitative proteomics of transporter expression in brain capillary endothelial cells isolated from P-glycoprotein (P-gp), breast cancer resistance protein (Bcrp), and P-gp/Bcrp knockout mice. *Drug Metab Dispos* **40**:1164–1169.

Allen JD, van Loevezijn A, Lakhai JM, van der Valk M, van Tellingen O, Reid G, Schellens JH, Koomen GJ, and Schinkel AH (2002) Potent and specific inhibition of the breast cancer resistance protein multidrug transporter in vitro and in mouse intestine by a novel analogue of fumitremorgin C. *Mol Cancer Ther* **1**:417–425.

Balogh LM, Kimoto E, Chupka J, Zhang H, and Lai Y (2013) Membrane protein quantification by peptide-based mass spectrometry approaches: studies on the organic anion-transporting polypeptide family. *J Proteomics Bioinform* **6**:229–236.

Di L, Rong H, and Feng B (2013) Demystifying brain penetration in central nervous system drug discovery. Miniperspective. *J Med Chem* **56**:2–12.

Doran A, Obach RS, Smith BJ, Hosea NA, Becker S, Callegari E, Chen C, Chen X, Choo E, Cianfrogna J, et al. (2005) The impact of P-glycoprotein on the disposition of drugs targeted for indications of the central nervous system: evaluation using the MDR1A/1B knockout mouse model. *Drug Metab Dispos* **33**:165–174.

Doyle L and Ross DD (2003) Multidrug resistance mediated by the breast cancer resistance protein BCRP (ABCG2). *Oncogene* **22**:7340–7358.

Doyle LA, Yang W, Abruzzo LV, Krogmann T, Gao Y, Rishi AK, and Ross DD (1998) A multidrug resistance transporter from human MCF-7 breast cancer cells. *Proc Natl Acad Sci USA* **95**:15665–15670.

Enokizono J, Kusuhara H, Ose A, Schinkel AH, and Sugiyama Y (2008) Quantitative investigation of the role of breast cancer resistance protein (Bcrp/Abcg2) in limiting brain and testis penetration of xenobiotic compounds. *Drug Metab Dispos* **36**:995–1002.

Enokizono J, Kusuhara H, and Sugiyama Y (2007) Effect of breast cancer resistance protein (Bcrp/Abcg2) on the disposition of phytoestrogens. *Mol Pharmacol* **72**:967–975.

Feng B, Mills JB, Davidson RE, Mireles RJ, Janiszewski JS, Troutman MD, and de Morais SM (2008) In vitro P-glycoprotein assays to predict the in vivo interactions of P-glycoprotein with drugs in the central nervous system. *Drug Metab Dispos* **36**:268–275.

Fuchs H, Kishimoto W, Gansser D, Tanswell P, and Ishiguro N (2014) Brain penetration of WEB 2086 (apafant) and dantrolene in Mdr1a (P-glycoprotein) and Bcrp knockout rats. *Drug Metab Dispos* **42**:1761–1765.

Hoshi Y, Uchida Y, Tachikawa M, Inoue T, Ohtsuki S, and Terasaki T (2013) Quantitative atlas of blood-brain barrier transporters, receptors, and tight junction proteins in rats and common marmoset. *J Pharm Sci* **102**:3343–3355.

Jablonski MR, Jacob DA, Campos C, Miller DS, Maragakis NJ, Pasinelli P, and Trotti D (2012) Selective increase of two ABC drug efflux transporters at the blood-spinal cord barrier suggests induced pharmacoresistance in ALS. *Neurobiol Dis* **47**:194–200.

Kalvass JC and Pollack GM (2007) Kinetic considerations for the quantitative assessment of efflux activity and inhibition: implications for understanding and predicting the effects of efflux inhibition. *Pharm Res* **24**:265–276.

Kamiie J, Ohtsuki S, Iwase R, Ohmine K, Katsukura Y, Yanai K, Sekine Y, Uchida Y, Ito S, and Terasaki T (2008) Quantitative atlas of membrane transporter proteins: development and application of a highly sensitive simultaneous LC/MS/MS method combined with novel in-silico peptide selection criteria. *Pharm Res* **25**:1469–1483.

Kikuchi R, de Morais SM, and Kalvass JC (2013) In vitro P-glycoprotein efflux ratio can predict the in vivo brain penetration regardless of biopharmaceutics drug disposition classification system class. *Drug Metab Dispos* **41**:2012–2017.

Kodaira H, Kusuhara H, Ushiki J, Fuse E, and Sugiyama Y (2010) Kinetic analysis of the cooperation of P-glycoprotein (P-gp/Abcb1) and breast cancer resistance protein (Bcrp/Abcg2) in limiting the brain and testis penetration of erlotinib, flavopiridol, and mitoxantrone. *J Pharmacol Exp Ther* **333**:788–796.

Kumar V, Prasad B, Patilea G, Gupta A, Salphati L, Evers R, Hop CE, and Unadkat JD (2015) Quantitative transporter proteomics by liquid chromatography with tandem mass spectrometry: addressing methodologic issues of plasma membrane isolation and expression-activity relationship. *Drug Metab Dispos* **43**:284–288.

Kumata K, Ogawa M, Takei M, Fujinaga M, Yoshida Y, Nengaki N, Fukumura T, Suzuki K, and Zhang MR (2012) Radiosynthesis of [^{13}N]dantrolene, a positron emission tomography probe for breast cancer resistant protein, using no-carrier-added [^{13}N]ammonia. *Bioorg Med Chem* **20**:305–310.

Lee CA, O'Connor MA, Ritchie TK, Galetin A, Cook JA, Ragueneau-Majlessi I, Ellens H, Feng B, Taub ME, Paine MF, et al. (2015) Breast cancer resistance protein (ABCG2) in clinical pharmacokinetics and drug interactions: practical recommendations for clinical victim and perpetrator drug-drug interaction study design. *Drug Metab Dispos* **43**:490–509.

Liu H, Li Y, Lu S, Wu Y, and Sahi J (2014) Temporal expression of transporters and receptors in a rat primary co-culture blood-brain barrier model. *Xenobiotica* **44**:941–951.

Liu H, Yu N, Lu S, Ito S, Zhang X, Prasad B, He E, Lu X, Li Y, Wang F, et al. (2015) Solute carrier family of the organic anion-transporting polypeptides 1A2- Madin-Darby canine kidney II: a promising in vitro system to understand the role of organic anion-transporting polypeptide 1A2 in blood-brain barrier drug penetration. *Drug Metab Dispos* **43**:1008–1018.

Mahar Doan KM, Humphreys JE, Webster LO, Wring SA, Shampine LJ, Serabjit-Singh CJ, Adkison KK, and Polli JW (2002) Passive permeability and P-glycoprotein-mediated efflux differentiate central nervous system (CNS) and non-CNS marketed drugs. *J Pharmacol Exp Ther* **303**:1029–1037.

Peng KW, Bacon J, Zheng M, Guo Y, and Wang MZ (2015) Ethnic variability in the expression of hepatic drug transporters: absolute quantification by an optimized targeted quantitative proteomic approach. *Drug Metab Dispos* **43**:1045–1055.

Poguntke M, Hazai E, Fromm MF, and Zolk O (2010) Drug transport by breast cancer resistance protein. *Expert Opin Drug Metab Toxicol* **6**:1363–1384.

Poirier A, Portmann R, Cascais AC, Bader U, Walter I, Ullah M, and Funk C (2014) The need for human breast cancer resistance protein substrate and inhibition evaluation in drug discovery and development: why, when, and how? *Drug Metab Dispos* **42**:1466–1477.

Prasad B and Unadkat JD (2015) The concept of fraction of drug transported (f_t) with special emphasis on BBB efflux of CNS and antiretroviral drugs. *Clin Pharmacol Ther* **97**:320–323.

Schinkel AH, Wagenaar E, Mol CA, and van Deemter L (1996) P-glycoprotein in the blood-brain barrier of mice influences the brain penetration and pharmacological activity of many drugs. *J Clin Invest* **97**:2517–2524.

Schnepf R and Zolk O (2013) Effect of the ATP-binding cassette transporter ABCG2 on pharmacokinetics: experimental findings and clinical implications. *Expert Opin Drug Metab Toxicol* **9**:287–306.

Shawahna R, Uchida Y, Declèves X, Ohtsuki S, Yousif S, Dauchy S, Jacob A, Chassoux F, Daumas-Duport C, Couraud PO, et al. (2011) Transcriptomic and quantitative proteomic analysis of transporters and drug metabolizing enzymes in freshly isolated human brain microvessels. *Mol Pharm* **8**:1332–1341.

Shen S and Zhang W (2010) ABC transporters and drug efflux at the blood-brain barrier. *Rev Neurosci* **21**:29–53.

Shepard RL, Cao J, Starling JJ, and Dantzig AH (2003) Modulation of P-glycoprotein but not MRP1- or BCRP-mediated drug resistance by LY335979. *Int J Cancer* **103**:121–125.

Tachibana T, Kitamura S, Kato M, Mitsui T, Shirasaka Y, Yamashita S, and Sugiyama Y (2010) Model analysis of the concentration-dependent permeability of P-gp substrates. *Pharm Res* **27**:442–446.

Uchida Y, Ohtsuki S, Kamiie J, and Terasaki T (2011a) Blood-brain barrier (BBB) pharmacoproteomics: reconstruction of in vivo brain distribution of 11 P-glycoprotein substrates based on the BBB transporter protein concentration, in vitro intrinsic transport activity, and unbound fraction in plasma and brain in mice. *J Pharmacol Exp Ther* **339**:579–588.

Uchida Y, Ohtsuki S, Katsukura Y, Ikeda C, Suzuki T, Kamiie J, and Terasaki T (2011b) Quantitative targeted absolute proteomics of human blood-brain barrier transporters and receptors. *J Neurochem* **117**:333–345.

Uchida Y, Tachikawa M, Obuchi W, Hoshi Y, Tomioka Y, Ohtsuki S, and Terasaki T (2013) A study protocol for quantitative targeted absolute proteomics (QTAP) by LC-MS/MS: application for inter-strain differences in protein expression levels of transporters, receptors, claudin-5, and marker proteins at the blood-brain barrier in ddY, FVB, and C57BL/6J mice. *Fluids Barriers CNS* **10**:21.

Uchida Y, Wakayama K, Ohtsuki S, Chiba M, Ohe T, Ishii Y, and Terasaki T (2014) Blood-brain barrier pharmacoproteomics-based reconstruction of the in vivo brain distribution of P-glycoprotein substrates in cynomolgus monkeys. *J Pharmacol Exp Ther* **350**:578–588.

Xiong H, Callaghan D, Jones A, Bai J, Rasquinha I, Smith C, Pei K, Walker D, Lue LF, Stanimirovic D, et al. (2009) ABCG2 is upregulated in Alzheimer's brain with cerebral amyloid angiopathy and may act as a gatekeeper at the blood-brain barrier for $A\beta_{1\text{-}40}$ peptides. *J Neurosci* **29**:5463–5475.

Yamazaki M, Neway WE, Ohe T, Chen I, Rowe JF, Hochman JH, Chiba M, and Lin JH (2001) In vitro substrate identification studies for P-glycoprotein-mediated transport: species difference and predictability of in vivo results. *J Pharmacol Exp Ther* **296**:723–735.

Zhao R, Raub TJ, Sawada GA, Kasper SC, Bacon JA, Bridges AS, and Pollack GM (2009) Breast cancer resistance protein interacts with various compounds in vitro, but plays a minor role in substrate efflux at the blood-brain barrier. *Drug Metab Dispos* **37**:1251–1258.

Zhou L, Schmidt K, Nelson FR, Zelesky V, Troutman MD, and Feng B (2009) The effect of breast cancer resistance protein and P-glycoprotein on the brain penetration of flavopiridol, imatinib mesylate (Gleevec), prazosin, and 2-methoxy-3-(4-(2-(5-methyl-2-phenyloxazol-4-yl)ethoxy)-phenyl)propanoic acid (PF-407288) in mice. *Drug Metab Dispos* **37**:946–955.

Address correspondence to: Houfu Liu, GlaxoSmithKline R&D China, 898 Halei Road, Zhangjiang Hi-Tech Park, Shanghai 201203, China. E-mail: hofmann.h.liu@gsk.com